Theoret. chim. Acta (Berl.) 19, 20—37 (1970)

A Non-Empirical Study of the Hydrogen Bond between Peptide Units

M. DREYFUS and A. PULLMAN
Institut de Biologie Physico-Chimique, 13, rue P. et M. Curie, Paris 5è

Received June 10, 1970

A detailed study of hydrogen bonding in the linear dimers of formamide has been performed in a non-empirical SCF framework. The stabilization energy is studied as a function of the distance between the monomers and a decomposition of the energy into the coulomb, exchange and polarization and charge transfer contributions is given as well as a study of the underlying changes in the electron distribution. The angular displacements around the carbonyl oxygen are studied in the antiparallel dimer and show a very shallow minimum. The effects of hydrogen bonding on the NH stretching are satisfactorily accounted for.

Die Wasserstoffbindung in den linearen Dimeren des Formamids wird im Rahmen der nicht-empirischen SCF-Theorie behandelt. Die Stabilisierungsenergie wird als Funktion des Abstands der Monomeren untersucht. Dabei wird auch die Zerlegung der Energie in Coulomb-, Austausch-, Polarisations-Ladungsübertragungs-Anteile gegeben. Die dabei stattfindenden Änderungen in der Elektronenverteilung werden untersucht. Die winkelabhängigen Verschiebungen um das Sauerstoffatom der Carbonyl-Gruppe werden für das antiparallele Dimere untersucht und zeigen ein schwaches Minimum. Der Einfluß der Wasserstoffbindung auf die NH-Streckung wird befriedigend wiedergegeben.

Une étude détaillée de la liaison hydrogène dans les dimères linéaires de la formamide est faite par une méthode SCF non-empirique. L'énergie de stabilisation est étudiée en fonction de la distance entre les monomères et de l'angle des liaisons C=O et HN. Une décomposition de l'énergie en ses composantes coulombienne, d'échange et de polarisation plus transfert de charge a été faite ainsi qu'une étude concomittante des déplacements électroniques correspondants.

1. Introduction

During the past fifty years a considerable number of papers has been devoted to the theoretical study of the hydrogen bond. Although the emphasis has been at the beginning on electrostatic forces, it was soon recognized that short range repulsions played an important role and further that charge-transfer and polarization effects could not be ignored. However the respective roles and weights of these different contributions are still disputed [1]. Clearly this comes from the fact that, until very recently, calculations on the hydrogen bond were of a very approximate nature: because of the size of even the smallest hydrogen-bonded system, either the theoretical method had to be oversimplified, or the system studied had to be truncated. Owing to the recent development of larger computing facilities the situation is changing rapidly in the sense that the wave function of a complete hydrogen-bonded system including all the electrons in the field of all the nuclei can now be calculated in a non-empirical way in the framework of the LCAO MO SCF method [2]. Clearly the use of such procedures is a primary step towards a better understanding of the hydrogen bond.

The first calculation of this kind on a "weak" hydrogen bond was the study of the water dimer [3], lately refined in diverse ways [4–6] and now supplemented by calculations on the trimers [7, 8]. The NH_3–HCl-complex [9] and the system LiH–Li^+ [10] have equally been studied. We have ourselves performed a similar investigation on the hydrogen bond between peptide units and already reported the results concerning the cyclic dimer known to occur in formamide crystals [11]. We have now applied the same methods to the linear dimers I and II of formamide. Moreover, in the present study we have tried to go a step further in the understanding of the SCF results by performing a decomposition of the stabilization energy into Coulomb, exchange, polarization and charge transfer contributions which refer to familiar notions. The point of view adopted is exposed in the next section together with the procedures.

2. Standpoint and Methods

The primary procedure adopted here as in our provious work [11] is to treat the hydrogen-bonded dimer as a single supermolecular system by the LCAO self-consistent procedure of Roothaan [2]. A measure of the hydrogen-bond energy is thus obtained as the difference between the SCF dimer energy and twice the energy of a single isolated monomer calculated in the same fashion. This SCF energy can be decomposed into different contributions, so as to make appear in particular those which would be obtained in a first-order perturbation treatment: let Ψ_M^0 be the SCF wave function of the isolated monomer, and suppose that we use as zeroth-order wave function for the dimer a *simple product:*

$$\Psi^0 = \Psi_{M_1}^0 \Psi_{M_2}^0 . \tag{1}$$

In that case the first order perturbation energy upon dimer formation would simply be the Coulomb energy E_C between the unperturbed charge distributions on the monomers M_1 and M_2.

If, in a better approach for overlapping molecules [12–14] one takes as zeroth-order wave function an antisymmetrized product of the monomer wave functions:

$$\Psi_A^0 = \mathscr{A}[\Psi_{M_1}^0 \Psi_{M_2}^0] , \tag{2}$$

where $\mathscr{A}$ is the antisymmetrizer operator, the first-order energy would become:

$$E^1 = E_C + E_E \tag{3}$$

where E_E is the exchange energy due to antisymmetrization.

It has been suggested recently [15] that E^1 could be obtained quite easily as a sub-product of an SCF treatment of the dimer when using as trial vectors the SCF molecular orbitals of the isolated monomers. At the first iteration the dimer wave function is indeed simply the antisymmetrized product (2) and E^1 is the corresponding energy. We have taken advantage of this suggestion and calculated E^1 in this way.

Moreover, we have thought interesting to go deeper into the decomposition of E^1 itself by computing its Coulomb part E_C. This may be done exactly using the expression:

$$E_C = -2\sum_i \sum_\nu Z_\nu \int \frac{|\varphi_i(1)|^2 \, d\tau_1}{r_{1\nu}} - 2\sum_j \sum_\mu Z_\mu \frac{|\varphi_j(2)|^2 \, d\tau_2}{r_{2\mu}} + 4\sum_i \sum_j \int \frac{|\varphi_i(1)|^2 \, |\varphi_j(2)|^2}{r_{12}} d\tau_1 d\tau_2 + \sum_\mu \sum_\nu \frac{Z_\mu Z_\nu}{r_{\mu\nu}}, \tag{4}$$

where μ and φ_i are the nuclei and unperturbed MO of monomer M_1, ν and φ_j those of monomer M_2. All the integrals have been computed exactly in terms of integrals over atomic orbitals[1]. Thus the exchange part of the first-order energy can be obtained by the difference:

$$E_E = E^1 - E_C . \tag{5}$$

The next step is the comparison between the first-order energy and the global SCF energy that we called E_{SCF}. This represents the extra stabilization obtained when pursuing the iteration procedure on the dimer until completion. Thus it accounts on the one hand for polarization and delocalization induced in one unit by the permanent electric field of the other, and on the other hand for the consequences of modifications in the intramolecular field itself by the charge modifications due to antisymmetrization. Globally this can be denoted polarization + charge-transfer effects:

$$E_{P+CT} = E_{SCF} - E^1 . \tag{6}$$

As to the practical computations, they have been performed with the CDC 3600 version [16] of the IBMOL program [17]. The Gaussian basis set utilized throughout is the same as that already used for the cyclic dimer (set *B* of Ref. [11]) and for the study of large heterocycles [18]. The main features of this basis set and its validity compared to others have been studied elsewhere [11, 18, 19]. Exponents and contraction coefficients can be found in Ref. [18].

The dimer of formamide is an already quite large system for SCF computations (48 electrons); and the number of parameters needed to fix the position of one molecule with respect to the other is also large. Therefore, for obvious practical reasons, no geometrical optimization was attempted: the two interacting molecules were supposed to keep a constant geometry and the dimerization energy was calculated with respect to the energy of the two monomers at infinite separation "frozen" in the same geometry as in the dimer. Furthermore as the dimer of formamide is a model for the NH...O=C hydrogen-bond in proteins we have restricted ourselves to the conformations corresponding to the structures β-antiparallel (I) and parallel (II) occuring in fibrous proteins. The geometry for each unit was taken from X-rays studies of formamide crystals [20] as in our previous work [11]. Reasonable geometrical parameters were assumed for the hydrogens: 1.0 and 1.09 Å bond lengths for NH and CH bonds respectively.

[1] We wish to thank MM. Levy and Millié for their programming help in this part.

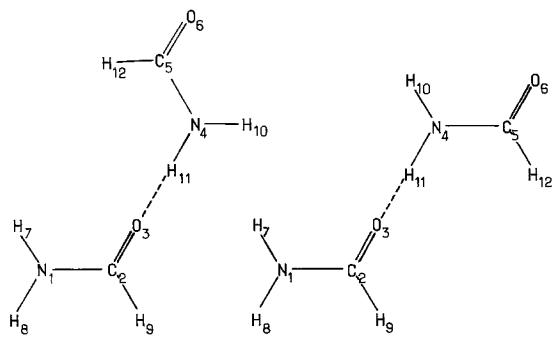

I II

First, the linear structures I and II have been examined and the O...N distance was varied. The results are presented in section 3. Sections 4 and 5 are concerned with the antiparallel dimer only, the O...N distance being held fixed at the equilibrium distance found in section 3. In section 4 the C=O...H angle was allowed to vary, fixing O...HN in a linear configuration (see Fig. 8). In section 5, the H-bonded proton was allowed to move along the O...N line, in order to find the NH bond length of minimum energy. A similar optimization was carried out for the isolated monomer and possible conclusions about H-bonding effect on the spectroscopic properties of NH bonds are discussed.

3. Analysis of the Hydrogen-Bond Energy and the Underlying Electron Displacements

The energy of the dimer I was computed for five values of the N...O distance. A computation of the energy of the parallel dimer II was made, the O...N distance being fixed at the minimum found for the antiparallel dimer. The results for the previously defined quantities, E_{SCF}, E^1, E_C and E_E are given in Table 1 and Fig. 1.

Table 1. *Energy of the antiparallel dimer I, and* H *bond energy as a function of the* O...N *distance. (The energy of the parallel dimer II has been computed only for* O...N = *2.85 Å, and is found to be −328.910652 a.u.)*

Distance O...N (Å)	2.65	2.85	3.05	3.25	5	∞
Antiparallel dimer SCF energy (atomic units)	−328.908174	−328.910607	−328.909970	−328.908339	−328900.765	−328.897952
H bonding energy (kcal/mol)	6.41	7.94	7.54	6.52	1.77	0

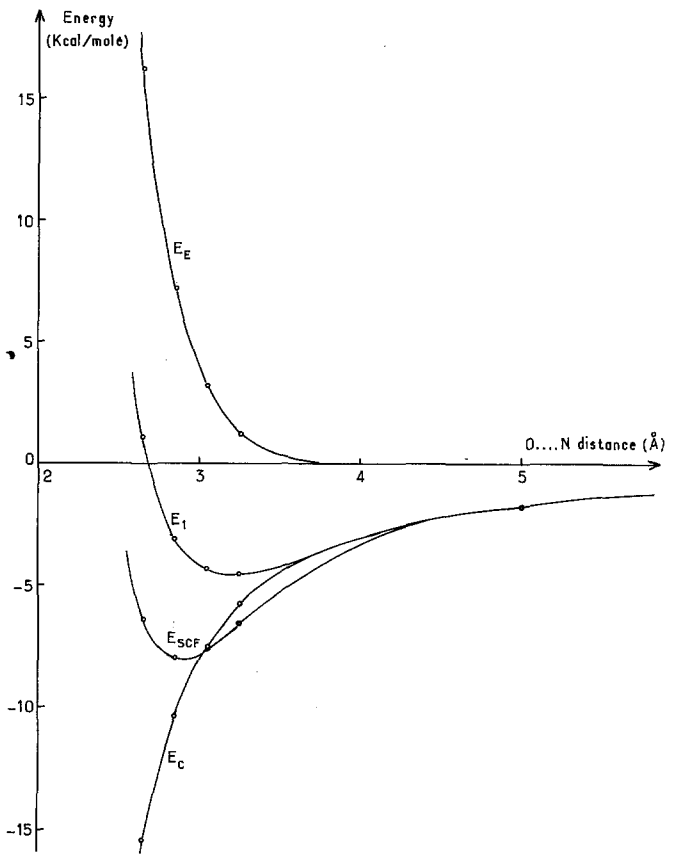

Fig. 1. Variation of the different energy components with the O...N distance (conformation I). Coulomb energy (E_C), exchange energy (E_E), their sum (E^1) and SCF interaction energy (E_{SCF}) are plotted as a function of the O...N distance (antiparallel dimer: see I) (kcal)

a) Coulomb and Exchange Terms

The first-order energy E^1 shows a value of 4.5 kcal/mole at the minimum of the curve, for an O...N distance of 3.2 Å (Fig. 1, E^1). As expected, its two components have opposite signs.

The coulomb energy is seen to decrease very slowly for long distances: for an O...N separation of 5 Å, its value is still 1.8 kcal/mol. At short intermolecular separation, E_C increases dramatically when decreasing O...N (Fig. 1) because of the interpenetration of the charge clouds [22, 15]. (The magnitude of this penetration part of E_C has been estimated[2] in a rather accurate way, it is zero for an O...N separation larger than 3.5 Å, and it increases exponentially below this distance; however, it is found to be only 20% of the total E_C at the SCF equilibrium distance, 2.85 Å.)

The variation of the exchange energy is also shown on the upper curve (Fig. 1). This contribution is zero at large intersystem separation and increases very

[2] See Ref. [21] for details.

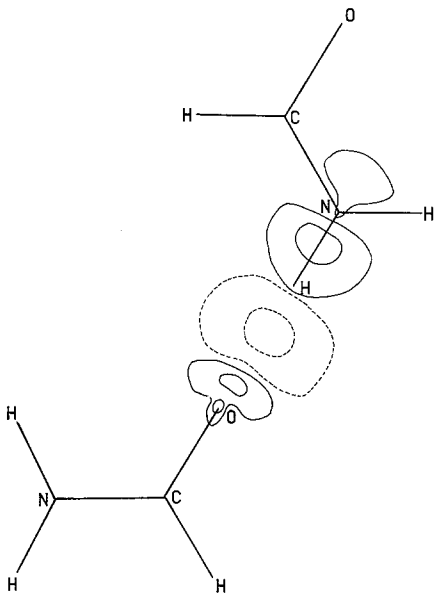

Fig. 2. Effect of antisymmetrization on electron density. This pictures the difference between the electron density associated with the antisymmetrized product of the wave functions for the separate monomers and the simple sum of the unperturbed densities. Dashed lines = loss of electronic charge; full lines = gain. Contours correspond to $\pm 10^{-3}$ and $\pm 5 \times 10^{-3}$ e/au^3. This map was drawn at an O... N distance of 2.65 Å, so as to emphasize the variations. The effect is qualitatively the same at the equilibrium distance, only smaller

rapidly when O... N is reduced; it becomes non-negligible for separations of about 3.5 Å, a value close to the sum of the Van der Waals radii of the atoms involved.

Salem [23] has suggested a useful interpretation of the exchange forces in terms of the changes in electron densities brought about by the sole antisymmetrization. To obtain a picture of these changes, we have drawn in Fig. 2 the density difference map of

$$\Delta\varrho = \varrho_{\text{antisymmetrized}} - \varrho_{\text{unperturbed}} \tag{7}$$

all over the dimer. In this expression $\varrho_{\text{unperturbed}}$ is obtained as $\sum_i 2\varphi_i^2$, where φ_i is the set of molecular orbitals of the isolated monomers; on the other hand, calling $\mathbf{S}$ the overlap matrix built with the φ_i's one can build a set of orthonormal molecular orbitals Ψ by:

$$\Psi = \mathbf{S}^{-1/2}\Phi \tag{8}$$

and $\varrho_{\text{antisymmetrized}}$ is obtained as $\sum_i 2\Psi_i^2$.

The figure obtained shows clearly that antisymmetrization of the wave function makes the electrons run away from the intersystem zone, with a piling-up of charge on each molecule. It is interesting to see that this electronic rearrangement is highly localized on the overlapping regions.

b) SCF *Results. Polarization and Charge-Transfer*

When the SCF procedure is carried out to its completion, the minimum energy is increased to 7.95 kcal/mol, for an O...N distance of 2.85 Å (Fig. 1). This equilibrium distance seems reasonnable but it must be recalled that attractive dispersion energy is not included in an SCF treatment: if it were, the equilibrium distance would become too short and the H bond energy would be larger. This is possibly due to an underestimation of the repulsion which seems to be quite sensitive to the quality of the atomic basis set [15].

A Mulliken-type population analysis [24] has been performed at various O...N distances. In Figs. 3 and 4 we have plotted the differences in atomic populations between dimer and monomer in terms of the intermolecular separation. In Fig. 4 we show also the global transfer of population from the proton acceptor to the proton donor. These diagrams indicate two interesting features:

i) The pertubation of the atomic populations is already visible at large intermolecular distance. This indicates the long-range character of polarization.

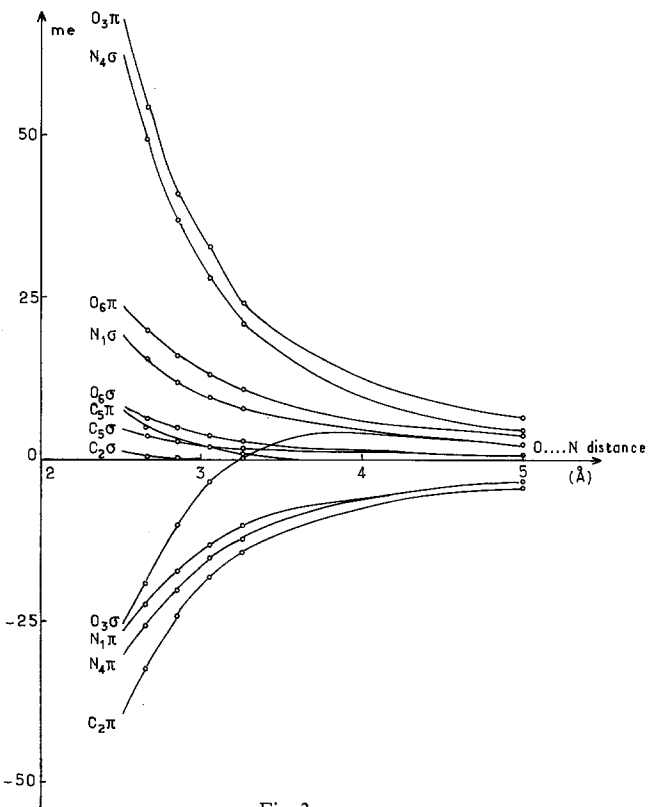

Fig. 3

Figs. 3 and 4. Variation of Mulliken atomic populations with the O...N distance. Positive ordinate correspond to a net gain of electrons (unity = 10^{-3} e) Fig. 3 deals with σ and π populations of the heavy atoms, Fig. 4 with the hydrogen populations; dashed line = variation of charge transfer

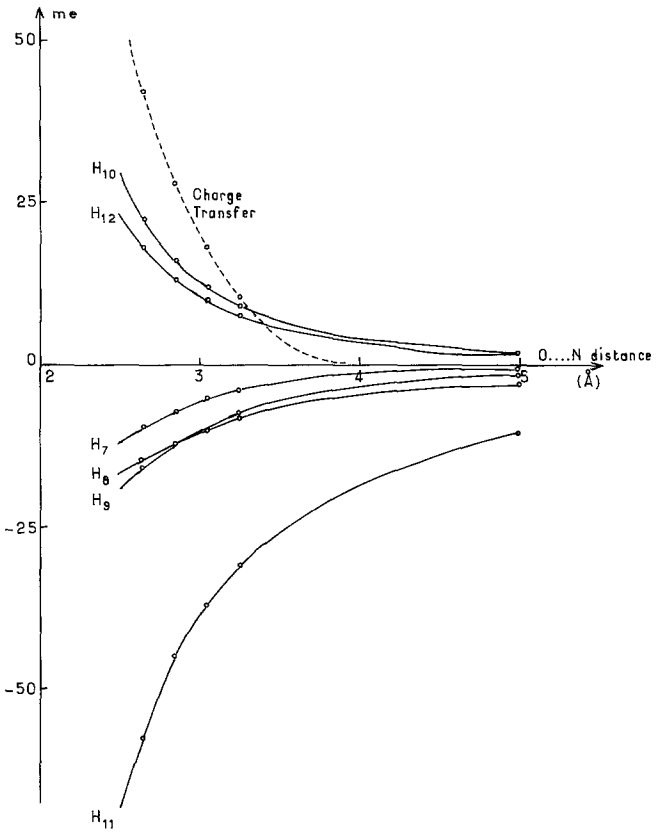

Fig. 4

ii) The variation of σ population of the proton-accepting atom, O_3 shows an inversion of sign when the O...N distance decreases: at large intermolecular separation, the electric field of the NH bond ($N^{\delta-}$ $H^{\delta+}$) polarizes the C=O bond and the oxygen population increases (both σ and π), the more labile π electrons being more affected. At shorter intermolecular separation (below 4 Å) this field induces charge transfer from the oxygen lone-pair to the antibonding NH* orbital, thus resulting in a loss of σ electrons on O_3.

The global polarization + charge transfer effect is pictured in Fig. 5 which gives the map of the isodensity difference in the molecular plane:

$$\varrho_{\text{dimer}} - \varrho_{\text{antisymmetrized monomer}}.$$

It appears that the intermolecular region increases its population under this effect, probably owing to charge-transfer. The most important displacement is clearly the polarization of the NH-bond towards the nitrogen under the field of the approaching polar carbonyl group. Another important point is the fact that the charge reorganization corresponding to $E_{SCF} - E^1$ is delocalized over the entire molecules, whereas that corresponding to exchange repulsion was confined to the O...H–N "bond".

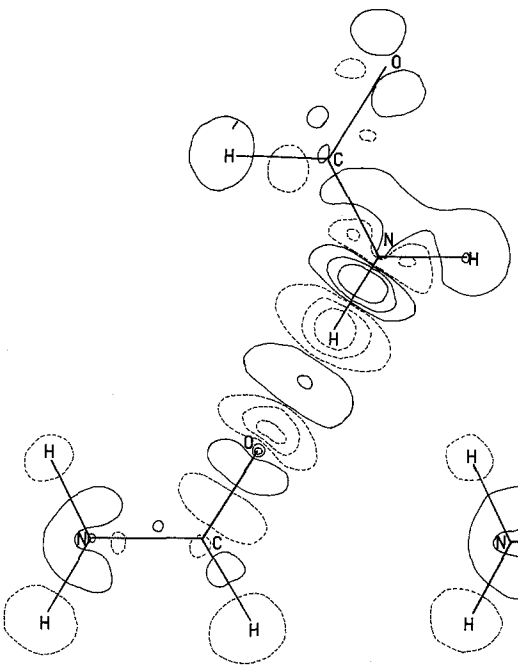

Fig. 5

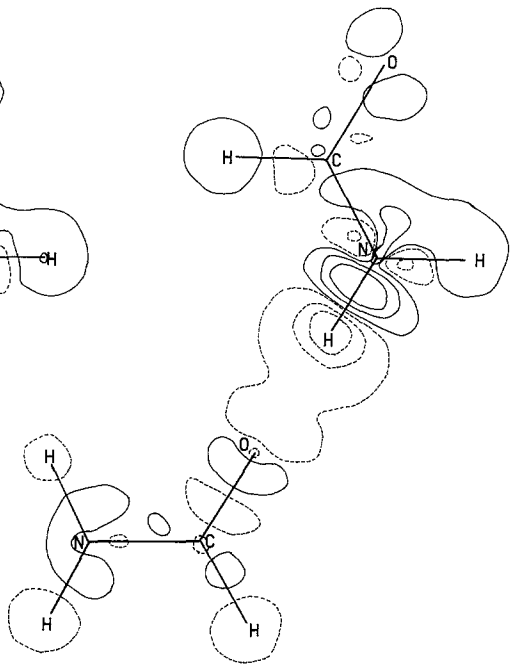

Fig. 6

Fig. 5. Difference of electronic density between the SCF dimer wave function and the antisymmetrized product of the SCF functions of the monomers. Dashed lines represent the regions inside which density is decreased by the SCF iterations, full lines represent the reverse situation. The values of these density difference are successively $\pm 10^{-3}$ (outor curves), $\pm 5 \times 10^{-3}$, $\pm 10^{-2}$, $\pm 2 \times 10^{-2}$ e/ua^3. The same conventions hold for the other differential density maps

Fig. 6. Global density difference map. This map shows the dimer electron density minus the sum of the densities of the isolated monomers with the same conventions as in Fig. 5

The global density difference between the dimer and the *isolated* monomers is given in Fig. 6; this corresponds to the global electronic effects upon hydrogen bonding[3]. It is seen that, as far as the O...H region is concerned the effect of charge-transfer is not important enough to cause a piling-up of electrons between the molecules, the reverse was observed in our previous study of the cyclic dimer [11] (see Sect. 4 for further discussion).

The global charge transfer observed at the equilibrium distance amounts to 29 millielectron units and this effect is practically entirely a σ transfer.

c) Ionization Potential and Dipole Moment Variation

In Fig. 7a and b we have plotted the variation of the highest occupied molecular orbital energy (homo) of the dimer and of the total dipole moment obtained in the SCF treatment, as a function of the distance of approach. The first quantity gives an approximation of the ionization potential (Koopmans' theorem).

[3] In order to make the comparison easier, the map of Fig. 6 is drawn like the two others, Figs. 2 and 5, for an O...N separation of 2.65 Å. The maps at the equilibrium distance show entirely similar features, although less pronounced.

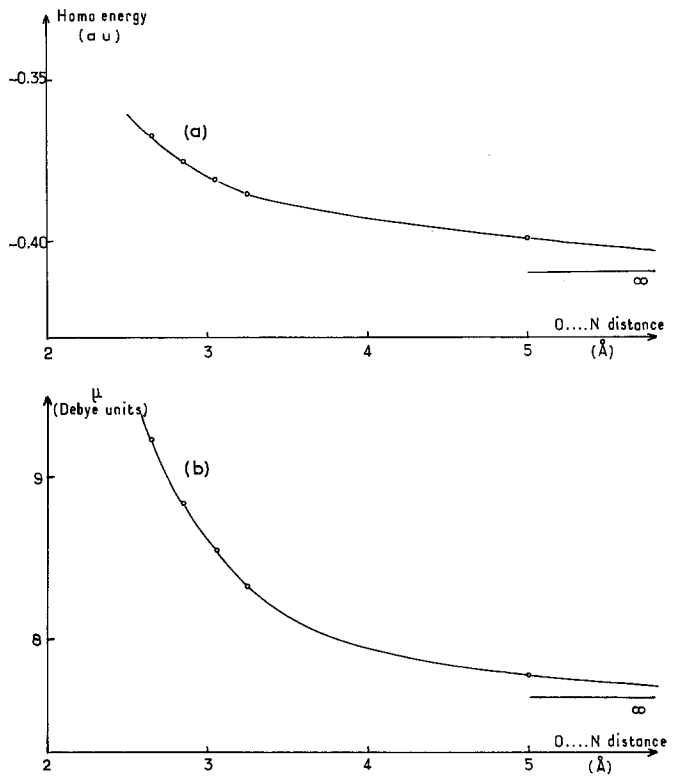

Fig. 7. a) Variation of the highest occupied molecular orbital energy of the proton-donating molecule, when the O...N distance is varied; b) same variation for the dipole moment of the complex

It is seen that the energy of the homo appears very sensitive to hydrogen bonding even at long distance. As in the monomer, the homo is a π orbital. In the dimer, the homo remains one of the two π orbitals of the proton-donor molecule; as polarization of the NH bond causes a piling-up if σ electrons on the nitrogen, the energy of the π level is raised. The highest σ occupied orbital in the dimer is made essentially of the O_6 oxygen lone-pairs; at infinite distance, its energy is only 0.3 eV above that of the π homo. For decreasing O...N distances this separation increases but both energies are raised. Thus both the π electron-donor ability and the *n* electron-donor ability should be increased by hydrogen-bonding, both properties being localized on the proton-donor unit. This has been also found recently for other complexes [4, 25] and confirms early conclusions by Suard *et al.* [26–28].

The dipole moment variation shows an enhancement with respect to the sum of the monomer dipoles. Although no experimental data is available on the formamide dimers, the effect seems reasonnable [29].

d) Parallel Dimer

SCF calculations have been performed on the parallel conformation of the linear dimer (II), with an O... N distance of 2.85 Å. The SCF energy (see Table 1),

the first order energy and the density difference maps differ so slightly from those of the antiparallel conformation that it seems that as far as hydrogen bonding is concerned, the two structures should have comparable stabilities. Thus we have pursued only the study of dimer I.

4. Angular Changes: Influence of the C–O...H Angle

This section deals with the angular variation shown in Fig. 8. The N...O distance was held fixed at a value of 2.85 Å, the energies and wave functions were computed for $\varphi = -45°$, 0°, +45°, +75°, and +90°. In fact, for $\varphi > 70°$ and $\varphi < -50°$, atoms others than those involved in the hydrogen bridge come within the sum of their Van der Waals radii so that studying the angular variation has little meaning outside these limits where the repulsion increases dramatically. Fig. 9 shows the energy variation in terms of the angle.

It is seen that the SCF curve has a very flat minimum between 45° and 75° and a slight shoulder for the linear arrangement. The decomposition of the energy into its components indicates that the electrostatic attraction E_C is quite dissymmetrical on each side of $\varphi = 0$, and is the source of the dissymmetry observed in E_{SCF}, the exchange repulsion variation as well as that of E_{P+CT} being symmetrical on each side of $\varphi = 0$. The variation of the exchange repulsion, E_E, with the angular displacement is rather large: it seems to show, among other things, that there is little hope to account accurately for the repulsion between nonbonded atoms with an expression taking into consideration only their distance, at least in the case of heteroatoms of non-spherical environment. In spite of its globally symmetrical aspect [11] the carbonyl oxygen presents a certain anisotropy of σ-electron density which is emphasized in Fig. 10. This is clearly related to the anisotropy in the repulsion energy.

Finally, the energy corresponding to polarization + charge transfer is minimal (in absolute value) for $\varphi = 0$ and increases on each side. An explanation of this fact is partially provided by the population analysis on the monomer: the highest occupied σ molecular orbital is practically a pure p lone-pair orbital, perpendicular to the CO bond, consequently the s-character of the lone-pair electrons facing the NH bond decreases from $\varphi = 0°$ to $\varphi = 90°$ so that their lability increases, thus favouring lone-pair delocalization terms. Indeed the charge transfer is 30% larger for $\varphi = 75°$ than for 0°.

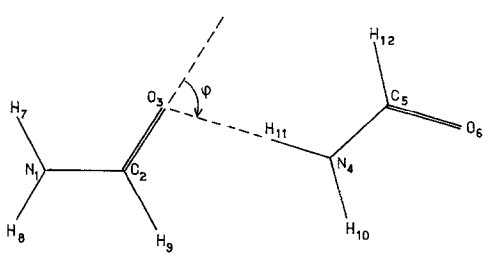

Fig. 8. Configuration of the dimer used for the angular variation in Section 4. The arrow shows positive sense choosen for φ in the text

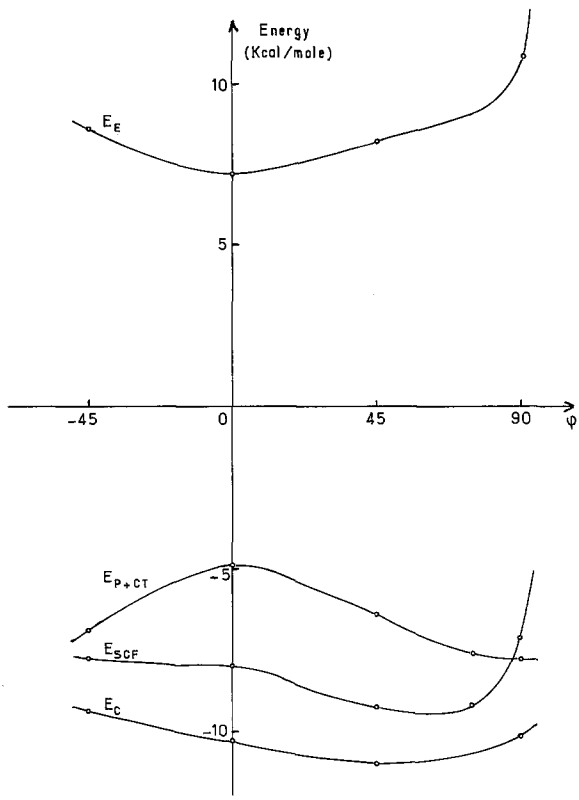

Fig. 9. Coulomb energy (E_C), Exchange energy (E_E), polarisation + charge transfer energy (E_{P+CT}) and SCF interaction energy (E_{SCF}), as a function of the angle φ (kcal/mol)

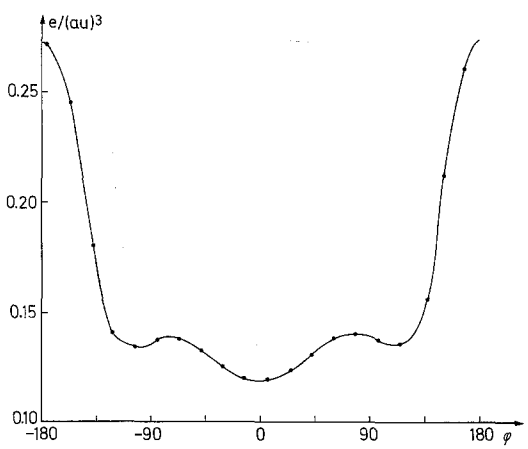

Fig. 10. Electron density at 1.5 ua from O_3, as a function of φ (e/A^3) (monomer, molecular plane)

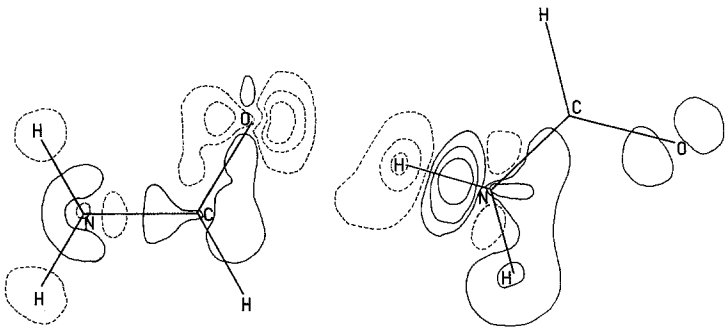

Fig. 11. Same as Fig. 6; but with $\varphi = 75°$

An isodifferential map is given in Fig. 11 for $\varphi = 75°$. It shows that polarization of the proton-donor is not much sensitive to φ. On the other hand it is clear that the oxygen lone-pair is much more delocalized than in the linear conformation. Apparently, some of this delocalization is at the advantage of the CO bond.

In conclusion, all contributions to the interaction energy are practically symmetrical on each side of $\varphi = 0$, *apart from the Coulomb energy*. The total energy is minimum for $\varphi \approx 60°$, but a large angular interval is within 1.5 kcal/mol above the minimum. This flatness results from conflicting variations of the different energy components. From a conformational point of view, the antiparallel dimer should adopt a conformation with positive φ, this being entirely due to simple electrostatics. And indeed, this is observed for instance in crystalline N methyl acetamide [30].

As to the flatness of the energy curve, it is in agreement with the fact recently outlined by Donohue [31] that the angular conditions required for hydrogen bonding to carbonyl groups do not seem to be as stringent as simple considerations on hybridization seemed to require. The previous discussion shows that considerations on the lone-pair direction alone are not sufficient to impose the direction of hydrogen bonding.

It is interesting to compare Fig. 11 with the similar map drawn for the cyclic dimer of formamide (Ref. [11], Fig. 4). A slight accumulation of electrons between O and H was observed, whereas it is not here, indicating that charge transfer was larger in the cyclic dimer then in the linear one. Furthermore, the electrostatic energy corresponding to the cyclic configuration is smaller than twice that observed in Fig. 9 for $\varphi = 60°$, but the exchange energy, depending only on the local overlap, is expected to be twice as large in the cyclic dimer as in our antiparallel dimer for $\varphi = 60°$. As the SCF H bonding energy was larger in the cyclic dimer than in any of our linear conformations E_{P+CT} was probably much larger. Apparently this is due to a cooperative effect: indeed, it is seen in Fig. 3 that both σ and π populations of the O_6 oxygen increase, as H bond is formed. Consequently, the O_6 lone pairs become more labile, and could form with another NH a bond stronger than the $O_3 \ldots H_{11}$ one.

5. Effect of Dimerization on the N–H Stretch

Hydrogen bonding AH... B is known to cause important modifications of the properties of the AH bond [29]. The AH stretching force constant is lowered (up to 10 to 20% in strong complexes); the AH equilibrium distance is lengthened, and the infrared intensity of the AH stretching band is usually dramatically increased.

Kollman and Allen have studied these spectroscopical properties of H bonding in $(H_2O)_2$ [4] and $(HF)_2$ [25] and shown that the SCF MO theory did give these effects at least qualitatively. We have performed a similar study on the linear antiparallel dimer.

The O... N distance was fixed at 2.85 Å and the hydrogen-bonded proton was allowed to move along the O... N line. A search for the equilibrium NH bond length was made in both the monomer and in the dimer, the NH bond direction being kept constant (Table 2). Assuming the energy to be a quadratic function of the NH distance, one finds an equilibrium value of 1.0617 Å in the monomer and 1.0718 in the dimer, thus an increase in length of 10^{-2} Å. The corresponding force constants are 0.488 and 0.474 atomic units respectively. The effects calculated are thus in the right direction although the numerical values by themselves should not be given too much significance.

What seems more interesting is to analyze how the different energy components contribute to these effects. Fig. 12 shows these variations. As may be expected the electrostatic energy becomes more attractive when the H...O distance is reduced, and the concavity of $E_C = f(\mathrm{NH})$ is negative. Thus, the electrostatic energy has the same influence on the equilibrium and force constant of the NH bond, as the total interaction energy, although quantitatively it leads to a larger Δr (0.02 Å), and Δk (−5%). This supports the ideas of Bader [32] that a purely electrostatic model should account, *at least qualitatively*, for these two properties of hydrogen bonding. However, Fig. 12 shows that the exchange energy increases when the H–N distance increases, and that its concavity is positive, so that this energy by itself would tend to shorten the NH bond and to increase its force constant. This effect may be immediatly understood when looking at Fig. 2: piling up of electrons in the NH bond and loss in the O... H region, cause a force on the H bonded proton directed towards the N atom.

In this range of intermolecular separation, the influence of the exchange energy prevails over the Coulomb energy, so that a first order treatment alone would predict a shortening of the NH bond, and an increase of its force constant.

Table 2. *Variation of the monomer and of the dimer I energy with the* N–H *bond length. In the dimer,* O... N *was fixed at 2.85 Å, and only the* NH *involved in the* H *bridge was varied*

NH (Å)	0.95	1.00	1.05	1.07	1.09
SCF energy (Monomer)	−164.438603	−164.448976	−164.452768	−164.452827	−164.452189
SCF energy (Dimer)	—	−328.901607	−328.915162	−328.915563	−328.915287

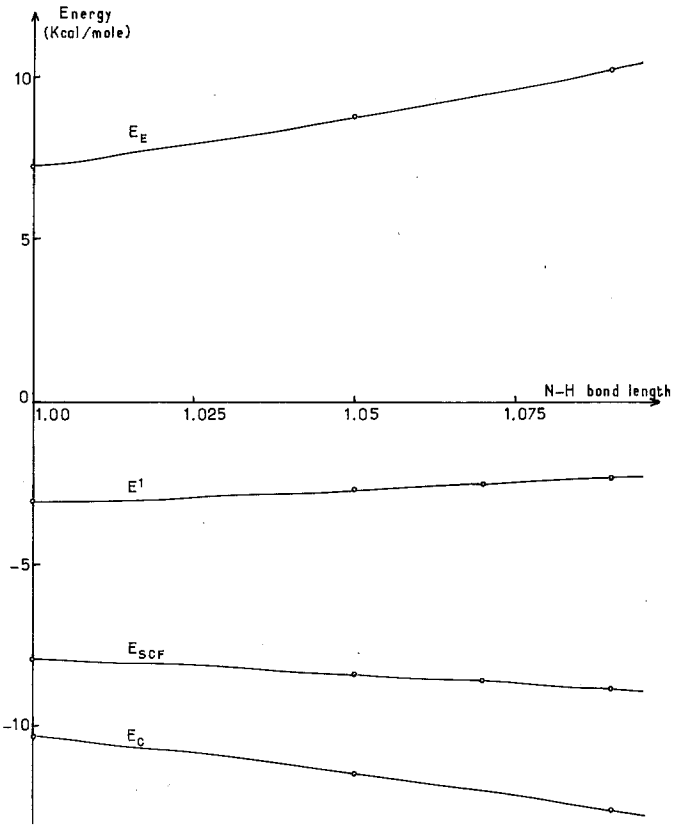

Fig. 12. Variation of the different energy components (kcal/mol), with the NH bond length (Å), with $\varphi = 0$ and O...N = 2.85 Å (Antiparallel dimer). E_C, E_E, E_{SCF} have the same meaning as before. $E^1 = E_C + E_E$ is the first order energy. All these components are computed with respect to the monomers in the same geometry

But the polarization + charge transfer energy reverses the situation; thus the observed overall effects are again the result of conflicting contributions from different energy components.

We have also evaluated the ratio of the integrated absorption intensity for the NH stretching mode in the dimer over that in the monomer, using the expression of the intensity [33]:

$$A = \frac{N\pi}{3c}\left(\frac{\partial \boldsymbol{\mu}}{\partial Q}\right)^2_{\text{eq}} \tag{9}$$

in terms of the total dipole moment $\boldsymbol{\mu}$ of the vibrating molecule (normal coordinate Q). Here Q was approximated by the NH distance r, $\boldsymbol{\mu}$ and its μ_x and μ_y components have been computed for each bond length (Table 3).

The ratio obtained was

$$\frac{A_{\text{dimer}}}{A_{\text{monomer}}} = 11.4 \tag{10}$$

Table 3. *Variation of the dipole moment vector for the monomer and for the dimer, when* NH *bond length is varied. The derivatives* $\left(\frac{\partial \mu_x}{\partial r}\right)_{eq}$ *and* $\left(\frac{\partial \mu_y}{\partial r}\right)_{eq}$ *were interpolated graphically. The last column leads to the ratio* $\left(\frac{\partial \mu}{\partial r}\right)^2_{eq\ dimer} \Big/ \left(\frac{\partial \mu}{\partial r}\right)^2_{eq\ mon} = 11.51$

All dipole moments are in Debye units	μ_x	μ_y	$\lvert\mu\rvert$	$\left(\frac{\partial \mu_x}{\partial r}\right)^a$	$\left(\frac{\partial \mu_y}{\partial r}\right)^a$	$\left(\frac{\partial \mu}{\partial r}\right)^{2\,a}$
Monomer						
NH = 1.0	−3.07890	−2.62337	4.04496			
NH = 1.05	−3.12572	−2.67630	4.11494	0.9255	1.0740	2.0100
NH = 1.07	−3.14423	−2.69778	4.14297			
NH = 1.09	−3.16270	−2.71951	4.17114			
Antiparallel dimer						
NH = 1.0	−4.50560	−7.60050	8.8356			
NH = 1.05	−4.60613	−7.79907	9.05771	2.2010	4.2775	23.1414
NH = 1.07	−4.65015	−7.88462	9.15376			
NH = 1.09	−4.69656	−7.97400	9.25432			

[a] At equilibrium distance.

Table 4. *Evaluation of the net charge transfer using Mulliken (1rst row), and Löwdin (2nd row) type population analysis, for two* NH *bond length*

Distance NH (Å)	1.00	1.09
Charge transfer (Mulliken)	29 mē	37.5 mē
Charge transfer (Löwdin)	29 mē	39 mē

a factor comparable to that obtained in Ref. [4] and of a plausible order of magnitude. When the NH bond vibrates, the distance form the oxygen lone-pair to the hydrogen varies causing a fluctuation of the charge transferred in phase with the vibration. This contributes to $\left(\frac{\partial \boldsymbol{\mu}}{\partial r}\right)_{eq}$ and it has been often assumed [34, 35] that this leads to the observed increase in intensity. We have evaluated this contribution to $\left(\frac{\partial \boldsymbol{\mu}}{\partial r}\right)_{eq}$, using the computed variation of the charge transfer during elongation (in order to avoid the well-known inconveniences of the Mulliken partition of overlap population, we have calculated the charge transfer both with Mulliken population and with a Löwdin population analysis [36] (Table 4). Interestingly enough, although the atomic population in both systematics are quite different, the amount of charge transferred is very similar within the two procedures).

Assuming that this transfer of charge could be located roughly from the oxygen to the middle of the NH bond, the contribution to $\frac{\partial \boldsymbol{\mu}}{\partial r}$ was calculated and added

vectorially to $\left(\frac{\partial \mu}{\partial r}\right)_{\text{monomer}}$ yielding

$$\left(\frac{\partial \mu}{\partial r}\right)^2_{\text{eq}} = 7.0\, D^2/\text{Å}^2 \tag{11}$$

whence an intensity ratio of 3.5, much smaller than the total value obtained directly, this indicating that charge transfer can account but for a part of the total intensity enhancement; the variation of the intramolecular polarization during vibration must also be considered. This is in agreement with Kollman and Allen's inferences [4].

6. Conclusions

This study shows that a reasonnable account of hydrogen bonding may be made on the basis of a non-empirical SCF treatment of the complete system. The decomposition of the energy into its components shows that for the formamide dimer, Coulomb attraction sets in at very large intermolecular separation whereas exchange repulsion effects come into play at about 3.7 Å intermolecular distance. The polarization and charge-transfer effects appreciably stabilize the complex and allow a closer approach of the two interacting molecules.

The study of the variation in the electron populations indicate that polarization begins at large distances (> 5 Å) whereas transfer of charges begins below 4 Å when the carbonyl oxygen of the proton-acceptor moiety starts to display a loss of σ electrons. The amount of charge transferred is very small and involves practically no π electrons. On the contrary charge reorganization inside each unit is important and involves both σ and π electrons.

Both exchange and polarization contribute to the overall electron displacements observed, the first effect being however confined to the O...HN part of the complex, whereas reorganization occurs throughout the two units. The high piling-up of electron density towards the proton-donor end of the A–H bond seems to be a characteristics of hydrogen-bonded systems [11, 25].

The angular variation of the interaction energy for the antiparallel dimer shows a very shallow minimum for a C=O...H angle of about 120°, the position of the minimum being essentially imposed by the Coulomb contribution. For the linear arrangement, the repulsion is minimum but the attractive polarization + charge transfer effect is also minimum, making the configuration less favoured.

The lengthening of the NH bond upon hydrogen-bonding also appears as the result of conflicting effects, exchange forces counteracting the lengthening contributed by Coulomb and polarization effects.

After this article was completed, we received in communication a preprint by P. A. Kollman and L. C. Allen where they make a partition of the hydrogen-bond energy into "electrostatic" and "delocalization" contributions. These corresponds to our E^1 and E_{P+CT}.

References

1. For a review of the pertinent literature, see Bratoz, S.: Advances quant. Chem. **3**, p. 209 (1967).
2. Roothan, C. C. J.: Rev. mod. Physics **23**, 69 (1951).
3. Morokuma, K., Pedersen, L.: J. chem. Physics **48**, 3275 (1968).
4. Kollman, P. A., Allen, L. C.: J. chem. Physics **51**, 3286 (1969).

5. Dirksen, G. H. F.: Chem. Physics Letters **4**, 373 (1969).
6. Morokuma, K., Winnick, J. R.: J. chem. Physics **52**, 1301 (1970).
7. Del Bene, J., Pople, J. A.: Chem. Physics Letters **4** (7), 426 (1969).
8. Hankins, D., Moskowitz, J. W.: Chem. Physics Letters **4** (9), 927 (1970).
9. Clementi, E.: J. chem. Physics **46**, 3851 (1967).
10. Dirksen, G., Preuss, H.: Int. J. quant. Chemistry **1**, 637 (1967).
11. Dreyfus, M., Maigret, B., Pullman, A.: Theoret. chim. Acta (Berl.) **17**, 109 (1970).
12. Eisenchitz, R., London, F.: Z. Physik **60**, 491 (1930).
13. Hirshfelder, J. O.: Chem. Physics Letters **1**, 325 (1967).
14. — Chem. Physics Letters **1**, 363 (1967).
15. Van Duijneveldt, F. B.: Thesis, Utrecht 1969.
16. Veillard, A., David, D. J., Millié, B.: Labo. Chim. ENS, Paris (1967).
17. Clementi, E., Davis, D. R.: J. comput. Physics **1**, 223 (1966).
18. Mély, B., Pullman, A.: Theoret. chim. Acta (Berl.) **13**, 278 (1969).
19. — Thèse 3è cycle. Paris (1969).
20. Ladell, J., Post, B.: Acta crystallogr. **7**, 559 (1954).
21. Dreyfus, M.: Thèse 3è cycle. Paris (1970).
22. Howard, B. B.: J. chem. Physics **39**, 2524 (1963).
23. Salem, L.: Proc. Roy. Soc. (London) A **264**, 379 (1961).
24. Mulliken, R. S.: J. chem. Physics **23**, 1833 (1955).
25. Kollman, P. A., Allen, L. C.: In press.
26. Suard, M., Berthier, G., Pullman, B.: Biochim. biophysica Acta **52**, 254 (1961).
27. — J. Chim. physique **62**, 79 (1965).
28. Pullman, B., Pullman, A.: Quant. Biochem. New York: Wiley-Interscience 1963.
29. Pimentel, G. C., McClellan, A. L.: The hydrogen bond, ed. by Freeman 1960.
30. Katz, J. L., Post, B.: Acta crystallogr. **13**, 624 (1960).
31. Donohue, J.: Structural chemistry and molecular biology, ed. by A. Rich and N. Davidson, p. 443. Freeman 1968.
32. Bader, R. F. W.: Canad. J. Chem. **42**, 1822 (1964).
33. Wilson, Jr., F. B., Decius, J. C., Cross, P. C.: Molecular vibrations. Mc Graw-Hill 1955.
34. Puranik, P. G., Kumar, V.: Proc. Indian Acad. Sci. **58** (1), p. 29 (1963).
35. Tsumobura, H.: J. chem. Physics **24**, 927 (1956).
36. Löwdin, P. O.: Adv. in Physics **5**, 22 p. 112 (1956).

Dr. A. Pullman
Institut de Biologie Physico-Chimique
13, rue P. et M. Curie
F-75 Paris 5è, France